Numerical analysis of two-phase fluid flow and heat transfer in porous media
by Matthew William Waite

A thesis submitted in partial fulfillment of the requirements for the degree of Master of Science in Mechanical Engineering
Montana State University
© Copyright by Matthew William Waite (1997)

Abstract:
Heat transfer and fluid flow in porous media have several important engineering applications. Among these applications are geothermal reservoirs, the dryout of moist organic soils due to forest or grass fires, and agricultural soil considerations. This study investigated transient and steady state heat and mass transfer of water with phase change in a homogeneous and isotropic Darcian porous medium heated from the side. The top surface was isothermal at atmospheric temperature, the lower surface was isothermal at an elevated temperature, while the left wall was adiabatic. The right side was subjected to a constant, uniform heat flux. The two vertical walls were impermeable, and the upper surface was maintained at a constant pressure. Fluid crossed the lower surface at a constant, uniform velocity.

The mathematical equations that govern two-phase fluid flow in porous media are highly nonlinear. In this study, these coupled nonlinear governing equations were solved using numerical methods. The energy equation was discretized and solved by using the control-volume based finite difference method. The continuity and momentum equations were combined, discretized, and solved using the error vector propagation method.

The resulting solutions were expressed in plots of constant temperature, streamlines, and velocity vectors. The parameters studied include the porous material, expressed as the Rayleigh number (Ra), the imposed side heat flux, the bottom surface temperature, and the bottom surface permeability. The resulting isotherm, streamline, and velocity vector plots were studied, and conclusions were drawn regarding each parameter. Additionally, transient plots were run for several cases. These transient solutions provided additional insight into the current problem.

The results obtained show that the Rayleigh number is a significant parameter. As Ra was decreased, the porous material was less permeable, and there was a shift in heat transfer from convection to conduction. The result was more vapor formation and an overall hotter enclosure. As the imposed side heat flux was increased, there was more vapor formation, an enclosure with more fluid at or near the saturation temperature, and faster fluid motion. As the bottom surface temperature was increased, there was more vapor formation and more fluid was at or near the saturation temperature. A permeable bottom surface enhanced heat transport from the bottom surface upward through the enclosure.

NUMERICAL ANALYSIS OF TWO-PHASE FLUID FLOW AND HEAT TRANSFER IN POROUS MEDIA

by

Matthew William Waite

A thesis submitted in partial fulfillment
of the requirements for the degree

of

Master of Science

in

Mechanical Engineering

MONTANA STATE UNIVERSITY - BOZEMAN
Bozeman, Montana

April 1997

N378
W1349

APPROVAL

of a thesis submitted by

Matthew William Waite

This thesis has been read by each member of the thesis committee and has been found to be satisfactory regarding content, English usage, format, citations, bibliographic style, and consistency, and is ready for submission to the College of Graduate Studies.

Dr. Ruhul Amin _____ (Signature) 15 April 1997 (Date)

Approved for the Department of Mechanical and Industrial Engineering

Dr. Vic Cundy _____ (Signature) 4/15/97 (Date)

Approved for the College of Graduate Studies

Dr. Robert Brown _____ (Signature) 4/18/97 (Date)

STATEMENT OF PERMISSION TO USE

In presenting this thesis in partial fulfillment of the requirements for a master's degree at Montana State University - Bozeman, I agree that the Library shall make it available to borrowers under rules of the Library.

If I have indicated my intention to copyright this thesis by including a copyright notice page, copying is allowable only for scholarly purposes, consistent with "fair use" as prescribed in the U. S. Copyright Law. Requests for permission for extended quotation from or reproduction of this thesis in whole or in parts may be granted only by the copyright holder.

Signature Matt Willen Wat

Date April 15, 1997

ACKNOWLEDGMENTS

I would like to thank Dr. Ruhul Amin for his guidance in my thesis work. I would also like to thank Dr. Thomas Reihman and Dr. Alan George for their support as committee members. I would also like to express my appreciation to Dr. C. Y. Wang for the initial version of the computer code used in this study.

My appreciation goes to the Department of Mechanical and Industrial Engineering for providing me with financial assistance. I would also like to thank my fellow graduate students and the staff of the Department of Mechanical and Industrial Engineering, whose support made this project successful, enjoyable, and rewarding.

TABLE OF CONTENTS

Page

LIST OF TABLES vii

LIST OF FIGURES viii

NOMENCLATURE xiii

ABSTRACT xvii

INTRODUCTION 1
- Motivation for Present Research 4
- Problem Description 5
- Literature Survey 8
  - General References 8
  - Fluid Flow in Porous Media 9
  - Two-Phase Flow in Porous Media 11
  - Two-Phase Flow Using Two-Phase Mixture Model 14
  - Experimental Studies in Porous Media Fluid Flow 15

PROBLEM FORMULATION 17
- Introduction 17
- Governing Equations 18
- Initial and Boundary Conditions 26
- Normalizing the Governing Equations 31

NUMERICAL METHOD 35
- Introduction 35
- Computational Grid 39
- Computational Matrix 42
- Validation of the Numerical Method 44

TABLE OF CONTENTS-continued

RESULTS AND DISCUSSION 49
Introduction 49
Effect of Side Imposed Heat Flux 53
Sand - High Permeability Porous Media (Ra=160) 54
Glass Beads- Medium Permeability Porous Media (Ra=56) 71
Soil - Low Permeability Porous Media (Ra=10) 83
Effect of Bottom Surface Temperature 94
Sand - High Permeability Porous Media (Ra=160) 95
Glass Beads- Medium Permeability Porous Media (Ra=56) 101
Soil - Low Permeability Porous Media (Ra=10) 106
Effect of Incoming Fluid Velocity at the Bottom Surface 111
Sand - High Permeability Porous Media (Ra=160) 113
Glass Beads- Medium Permeability Porous Media (Ra=56) 119
Soil - Low Permeability Porous Media (Ra=10) 122
Effect of the Porous Material 126
Transient Solutions 127

CONCLUSIONS AND RECOMMENDATIONS 140
Conclusions 140
Recommendations 142

REFERENCES CITED 143

LIST OF TABLES

Table		Page
1.	Thermophysical Properties of Water	29
2.	Thermophysical Properties of Porous Materials	30
3.	Computational Matrix for the Current Study	43
4.	Summary of Results	138

LIST OF FIGURES

Figure — Page

1. Typical Porous Medium with Two-Phase Fluid 2
2. Geometry of Problem Studied 6
3. Main Calculation Grid 40
4. Staggered Calculation Grid 41
5. Experimental and Numerical Results for Volumetric Vapor Fraction 46
6. Numerical Results for Volumetric Vapor Fraction 48
7. Isotherm and Streamline Plots for the Case Ra=160, θ_B=0.7, $u_{y,B}^*$=0.0, and Q_W=1.0 55
8. Isotherms, Streamlines, and Velocity Vector Plots for the Case Ra=160, θ_B=0.7, $u_{y,B}^*$=0.0, and Q_W=20.0 59
9. Isotherms, Streamlines, and Velocity Vector Plots for the Case Ra=160, θ_B=0.7, $u_{y,B}^*$=0.0, and Q_W=35.0 61
10. Isotherm and Streamline Plots for the Case Ra=160, θ_B=1.0, $u_{y,B}^*$=0.0, and Q_W=1.0 64
11. Isotherm and Streamline Plots for the Case Ra=160, θ_B=1.0, $u_{y,B}^*$=0.0, and Q_W=25.0 65
12. Isotherm and Streamline Plots for the Case Ra=160, θ_B=1.0, $u_{y,B}^*$=0.0, and Q_W=30.0 67
13. Isotherm and Streamline Plots for the Case Ra=160, θ_B=1.0, $u_{y,B}^*$=0.0, and Q_W=35.0 68
14. Top Heat Flux versus Imposed Heat Flux for Ra=160 70

LIST OF FIGURES - continued

Figure — Page

15. Isotherm and Streamline Plots for the Case Ra=56, θ_B=0.7, $u_{y,B}^*$=0.0, and Q_W=1.0 72

16. Isotherm and Streamline Plots for the Case Ra=56, θ_B=0.7, $u_{y,B}^*$=0.0, and Q_W=20.0 73

17. Isotherm and Streamline Plots for the Case Ra=56, θ_B=0.7, $u_{y,B}^*$=0.0, and Q_W=35.0 75

18. Isotherm and Streamline Plots for the Case Ra=56, θ_B=1.0, $u_{y,B}^*$=0.0, and Q_W=1.0 76

19. Isotherm and Streamline Plots for the Case Ra=56, θ_B=1.0, $u_{y,B}^*$=0.0, and Q_W=20.0 77

20. Isotherm and Streamline Plots for the Case Ra=56, θ_B=1.0, $u_{y,B}^*$=0.0, and Q_W=35.0 78

21. Volumetric Vapor Fraction versus Imposed Heat Flux for Ra=56 81

22. Top Heat Flux versus Imposed Heat Flux for Ra=56 82

23. Isotherm and Streamline Plots for the Case Ra=10, θ_B=0.7, $u_{y,B}^*$=0.0, and Q_W=1.0 84

24. Isotherm and Streamline Plots for the Case Ra=10, θ_B=0.7, $u_{y,B}^*$=0.0, and Q_W=10.0 85

25. Isotherm and Streamline Plots for the Case Ra=10, θ_B=0.7, $u_{y,B}^*$=0.0, and Q_W=20.0 86

26. Isotherm and Streamline Plots for the Case Ra=10, θ_B=1.0, $u_{y,B}^*$=0.0, and Q_W=1.0 88

27. Isotherm and Streamline Plots for the Case Ra=10, θ_B=1.0, $u_{y,B}^*$=0.0, and Q_W=10.0 89

LIST OF FIGURES - continued

Figure		Page
28.	Isotherm and Streamline Plots for the Case Ra=10, θ_B=1.0, $u_{y,B}^*$=0.0, and Q_W=20.0	90
29.	Volumetric Vapor Fraction versus Imposed Heat Flux for Ra=10	92
30.	Top Heat Flux versus Imposed Heat Flux for Ra=10	93
31.	Isotherm and Streamline Plots for the Case Ra=160, θ_B=0.7, $u_{y,B}^*$=0.0, and Q_W=1.0	96
32.	Isotherm and Streamline Plots for the Case Ra=160, θ_B=1.0, $u_{y,B}^*$=0.0, and Q_W=1.0	97
33.	Isotherm and Streamline Plots for the Case Ra=160, θ_B=0.7, $u_{y,B}^*$=0.0, and Q_W=25.0	99
34.	Isotherm and Streamline Plots for the Case Ra=160, θ_B=1.0, $u_{y,B}^*$=0.0, and Q_W=25.0	100
35.	Isotherm and Streamline Plots for the Case Ra=56, θ_B=0.7, $u_{y,B}^*$=0.0, and Q_W=5.0	102
36.	Isotherm and Streamline Plots for the Case Ra=56, θ_B=1.0, $u_{y,B}^*$=0.0, and Q_W=5.0	103
37.	Isotherm and Streamline Plots for the Case Ra=56, θ_B=0.7, $u_{y,B}^*$=0.0, and Q_W=25.0	104
38.	Isotherm and Streamline Plots for the Case Ra=56, θ_B=1.0, $u_{y,B}^*$=0.0, and Q_W=25.0	105
39.	Isotherm and Streamline Plots for the Case Ra=10, θ_B=0.7, $u_{y,B}^*$=0.0, and Q_W=5.0	107
40.	Isotherm and Streamline Plots for the Case Ra=10, θ_B=1.0, $u_{y,B}^*$=0.0, and Q_W=5.0	108

LIST OF FIGURES - continued

Figure — Page

41. Isotherm and Streamline Plots for the Case Ra=10, θ_B=0.7, $u_{y,B}^*$=0.0, and Q_W=15.0 109

42. Isotherm and Streamline Plots for the Case Ra=10, θ_B=1.0, $u_{y,B}^*$=0.0, and Q_W=15.0 110

43. Isotherm and Streamline Plots for the Case Ra=160, θ_B=0.7, $u_{y,B}^*$=0.0, and Q_W=10.0 114

44. Isotherm and Streamline Plots for the Case Ra=160, θ_B=0.7, $u_{y,B}^*$=2.86, and Q_W=10.0 115

45. Isotherm and Streamline Plots for the Case Ra=160, θ_B=1.0, $u_{y,B}^*$=2.86, and Q_W=40.0 116

46. Isotherm and Streamline Plots for the Case Ra=160, θ_B=1.0, $u_{y,B}^*$=5.73, and Q_W=40.0 117

47. Isotherm and Streamline Plots for the Case Ra=56, θ_B=1.0, $u_{y,B}^*$=0.0, and Q_W=15.0 120

48. Isotherm and Streamline Plots for the Case Ra=56, θ_B=1.0, $u_{y,B}^*$=2.85, and Q_W=15.0 121

49. Isotherm and Streamline Plots for the Case Ra=10, θ_B=0.7, $u_{y,B}^*$=0.0, and Q_W=10.0 123

50. Isotherm and Streamline Plots for the Case Ra=10, θ_B=0.7, $u_{y,B}^*$=2.06, and Q_W=10.0 124

51. Isotherm and Streamline Plots for the Case Ra=10, θ_B=0.7, $u_{y,B}^*$=4.13, and Q_W=10.0 125

52. Plot of Q_T, Q_B, and ϵ_v versus time for the case Ra=160, θ_B=0.7, $u_{y,B}^*$=2.86, and Q_W=10.0 130

LIST OF FIGURES - continued

Figure Page

53. Plot of Q_T, Q_B, and ϵ_v versus time for the case Ra=160, θ_B=1.0, $u_{y,B}^*$=2.86, and Q_W=10.0 131

54. Plot of Q_T, Q_B, and ϵ_v versus time for the case Ra=160, θ_B=0.7, $u_{y,B}^*$=2.86, and Q_W=20.0 132

55. Plot of Q_T, Q_B, and ϵ_v versus time for the case Ra=10, θ_B=0.7, $u_{y,B}^*$=2.06, and Q_W=10.0 135

56. Plot of Q_T, Q_B, and ϵ_v versus time for the case Ra=10, θ_B=1.0, $u_{y,B}^*$=2.06, and Q_W=10.0 136

NOMENCLATURE

Symbol	Description	Units
A	aspect ratio of porous enclosure ($=L_y/L_x$)	-----
C_p	specific heat	J/kg·K
D(s)	capillary diffusion coefficient, Eq. (25)	m^2/s
f(s)	hindrance function, Eq. (22)	-----
g	gravitational acceleration	m/s^2
g	gravitational acceleration vector	m/s^2
h	enthalpy	J/kg
h_{fg}	latent heat of liquid-vapor phase change	J/kg
H	volumetric enthalpy	J/m^3
j	diffusive mass flux, Eq. (26)	$kg/m^2 \cdot s$
J(s)	J-function for capillary pressure, Eq. (24)	-----
k_r	relative permeability	-----
k_{eff}	effective thermal conductivity, Eq. (15)	W/m·K
K	absolute permeability	m^2
L_x	length in x (horizontal) direction	m
L_y	length in y (vertical) direction	m
Le_c	Lewis number of capillary diffusion $[=(\epsilon K)^{1/2}\sigma C_{pl}/\upsilon_f k_{eff}]$	-----
p	pressure	Pa
p_c	capillary pressure, Eq. (23)	Pa

NOMENCLATURE - continued

Symbol	Description	Units
q	heat flux	W/m^2
Q	dimensionless heat flux $\{= qL_y/[k_{eff}(T_{sat}-T_o)]\}$	-----
Ra	single-phase Rayleigh number $[= KL_y g\rho_l\beta_l(T_{sat}-T_o)C_{pl}/(\nu_l k_{eff})]$	-----
$Ra_{2\phi}$	two-phase Rayleigh number $[= KL_y g\rho_l C_{pl}/(\nu_l k_{eff})]$	-----
s	liquid saturation	-----
t	time	s
t^*	dimensionless time $[= t/(L_y^2/\alpha_{eff})]$	-----
T	temperature	°C
u	velocity vector	m/s
u_x	velocity in x (horizontal) direction	m/s
u_x^*	dimensionless velocity in x direction $(= u_x L_x/\alpha eff)$	-----
u_y	velocity in y (vertical) direction	m/s
u_y^*	dimensionless velocity in y direction $(= u_y L_y/\alpha_{eff})$	-----
x	coordinate in horizontal direction	m
X	dimensionless x coordinate $(= x/L_x)$	-----
y	coordinate in vertical direction	m
Y	dimensionless y coordinate $(= y/L_y)$	-----
Greek Symbols		
α_{eff}	effective thermal diffusivity $[= k_{eff}/(\rho_l C_{pl})]$	m^2/s

NOMENCLATURE - continued

Symbol	Description	Units
α_s	heat capacitance ratio (solid-liquid) [$= \rho_s C_{ps} / (\rho_l C_{pl})$]	-----
α_v	heat capacitance ratio (vapor-liquid) [$= \rho_v C_{pv} / (\rho_v C_{pv})$]	-----
β	thermal expansion coefficient	K^{-1}
γ_h	two phase advection correction coefficient, Eq. (12)	-----
Γ_h	effective diffusion coefficient, Eq. (14)	kg/m·s
$\Delta\rho$	density difference ($= \rho_l - \rho_v$)	kg/m^3
ϵ	porosity	-----
ϵ_v	volume fraction of vapor phase, Eq. (47)	-----
θ	dimensionless temperature [$= (T-T_o)/(T_{sat}-T_o)$]	-----
λ	relative mobility	-----
μ	dynamic viscosity ($=\rho\nu$)	Pa·s
ν	kinematic viscosity	m^2/s
ρ	density	kg/m^3
σ	surface tension	N/m
ψ	stream function	m^2/s
ψ^*	nondimensional stream function ($= \psi/\alpha_{eff}$)	-----
Ω	effective heat capacitance ratio, Eq. (13)	-----
Subscripts		
B	bottom	N/A

NOMENCLATURE - continued

Symbol	Description	Units
c	capillary	N/A
l	liquid phase	N/A
o	initial	N/A
sat	saturated state	N/A
T	top	N/A
v	vapor phase	N/A
W	wall	N/A
x	x (horizontal) direction	N/A
y	y (vertical) direction	N/A
κ	"kinetic" property	N/A

ABSTRACT

Heat transfer and fluid flow in porous media have several important engineering applications. Among these applications are geothermal reservoirs, the dryout of moist organic soils due to forest or grass fires, and agricultural soil considerations. This study investigated transient and steady state heat and mass transfer of water with phase change in a homogeneous and isotropic Darcian porous medium heated from the side. The top surface was isothermal at atmospheric temperature, the lower surface was isothermal at an elevated temperature, while the left wall was adiabatic. The right side was subjected to a constant, uniform heat flux. The two vertical walls were impermeable, and the upper surface was maintained at a constant pressure. Fluid crossed the lower surface at a constant, uniform velocity.

The mathematical equations that govern two-phase fluid flow in porous media are highly nonlinear. In this study, these coupled nonlinear governing equations were solved using numerical methods. The energy equation was discretized and solved by using the control-volume based finite difference method. The continuity and momentum equations were combined, discretized, and solved using the error vector propagation method.

The resulting solutions were expressed in plots of constant temperature, streamlines, and velocity vectors. The parameters studied include the porous material, expressed as the Rayleigh number (Ra), the imposed side heat flux, the bottom surface temperature, and the bottom surface permeability. The resulting isotherm, streamline, and velocity vector plots were studied, and conclusions were drawn regarding each parameter. Additionally, transient plots were run for several cases. These transient solutions provided additional insight into the current problem.

The results obtained show that the Rayleigh number is a significant parameter. As Ra was decreased, the porous material was less permeable, and there was a shift in heat transfer from convection to conduction. The result was more vapor formation and an overall hotter enclosure. As the imposed side heat flux was increased, there was more vapor formation, an enclosure with more fluid at or near the saturation temperature, and faster fluid motion. As the bottom surface temperature was increased, there was more vapor formation and more fluid was at or near the saturation temperature. A permeable bottom surface enhanced heat transport from the bottom surface upward through the enclosure.

INTRODUCTION

A study of heat transfer and fluid flow with liquid-vapor phase change in a porous medium heated from the side has several important engineering applications. Among these applications are geothermal systems, oil reservoir engineering, thermal energy storage, heat pipes, and post-accident analysis of nuclear reactors. Additional applications include the dryout of moist organic soil due to a forest or grass fire [Hungerford et el. (1995)] and agricultural considerations concerning soil [Hungerford et al. (1991)]. Recently, scientists and engineers have been investigating how fluid flow in porous media relates to thermal energy storage. As the world's supplies of fossil fuels dwindles, engineers have shown an increased interest in alternative means of energy storage and recovery.

Fluid flow in a porous medium is due to either forced or natural convection. Forced convection is caused by fluid moving due to an externally applied pressure difference. Natural, or free, convection is caused by buoyancy effects. Buoyancy is due to the combination of a fluid density gradient and a body force, usually gravity, that proportional to a fluid density gradient. The necessary density gradient can result from a temperature gradient in the fluid. The result of the buoyancy effect is fluid motion in which warm, light fluid rises and cool, heavy fluid falls.

In general, a porous medium is a material that consists of a solid matrix with an interconnected void [Nield and Bejan (1992)]. Usually the solid matrix is assumed to be

rigid, or undergoes only small deformations. The void spaces, or pores, allow one or more fluids to flow through the material. In two-phase flow, the void space can be shared by gases, liquids, or a combination of gas and liquid. A typical porous medium filled with a two-phase fluid is shown in Figure 1. The amount of void space relative to the volume of a porous enclosure can vary significantly from one material to another, and thus fluid flow and heat transfer characteristics change significantly from one material to another.

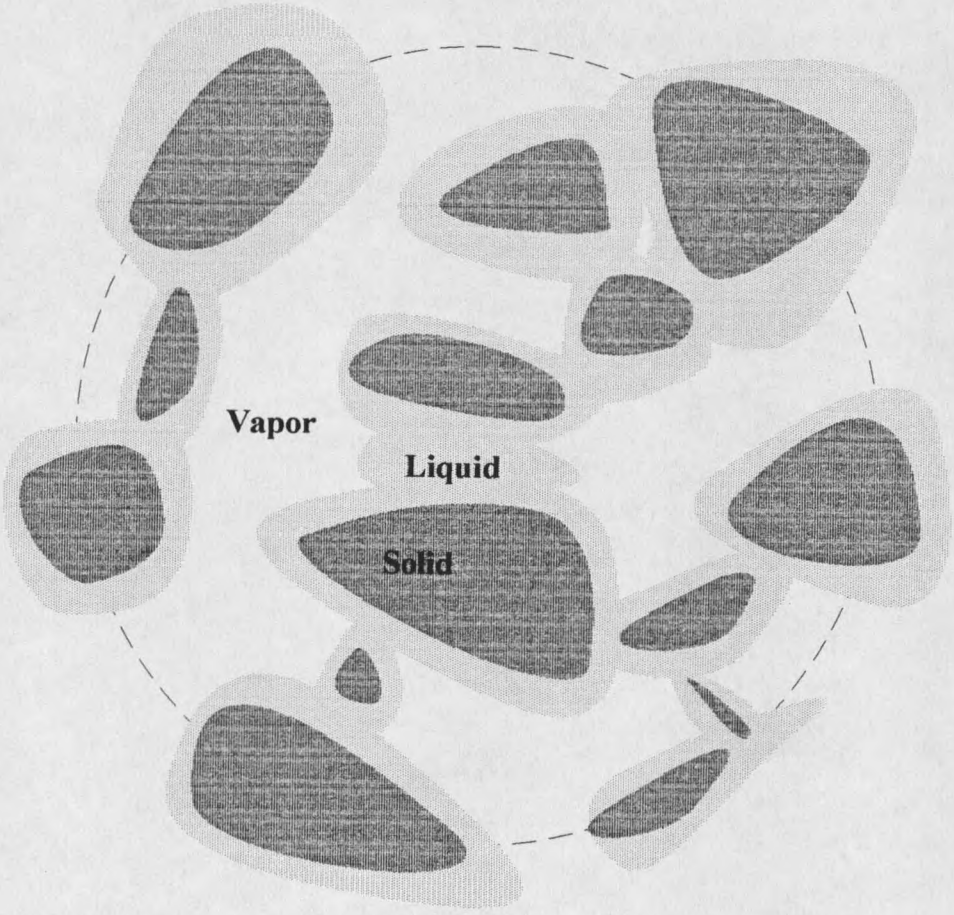

Figure 1. Typical Porous Medium With Two-Phase Fluid

Porous materials are in general defined by two quantities. These quantities, porosity and permeability, characterize the nature of fluid flow through porous media. Porosity is the fraction of total volume of the medium occupied by void space. Permeability is an empirical property that describes the ability of the porous medium to transmit fluid through it. In mathematical terms, permeability is the constant of proportionality between velocity (or mass flux) and the pressure gradient present in the porous enclosure. A high permeability porous medium allows easy, fast fluid motion, while a low permeability medium greatly restricts the motion of the fluid.

The mathematically expressed conservation equations that govern two-phase fluid flow in porous media are highly nonlinear. The equations are coupled and must be solved simultaneously. Therefore, analytical results are mostly limited to one-dimensional problems with several simplifying assumptions. For multi-dimensional problems governed by the complete conservation equations, such as most interesting engineering applications, numerical methods are the most common way to obtain solutions. The validity and accuracy of numerical methods are established by comparing numerical results with experimental results for the same case. After successful validation, the numerical methods can be satisfactorily extended to other situations.

Motivation for Present Research

The majority of previous research in porous media has been limited to single phase systems. Single phase studies limit the applicability of the research to situations in which the temperature is either significantly above or below the saturation temperature of the working fluid. For situations like geothermal reservoirs, temperature varies in such a range that studying the two-phase flow of the fluid is necessary. A typical geothermal reservoir consists of soil saturated with water at or near the boiling point.

Another interesting application of two-phase flow in porous media is that of oil reservoir engineering. In many underground oil reservoirs, the liquid crude oil may be mixed with another fluid such as natural gas. In such situations, the study of two-phase flow is valuable to determine the most effective method for crude oil extraction.

A porous enclosure heated from the side simulates many naturally occurring phenomena. Besides geothermal wells and oil reservoirs, such a study simulates the dryout of moist organic soil as a forest or grass fire passes through the region. The related application is the effect of heat and mass transfer on agricultural soils. If soil is heated above a certain temperature due to a forest fire, natural regrowth of the trees in that soil is not possible. So, the study of heat and mass transport of fluid in such media is essential.

Problem Description

Geometry of the problem analyzed is shown in Figure 2. The problem considered in this study consisted of a square, two-dimensional porous enclosure. The porous medium was assumed to be of uniform porosity and permeability. Initially, the enclosure was at ambient temperature and pressure and saturated with liquid water.

The thermal boundary conditions considered were as follows. The top surface was isothermal, at the ambient temperature. The bottom surface was isothermal, with various temperatures studied to cover a broad range of water temperatures in geothermal situations. The left wall was adiabatic and the right wall was subjected to a constant, uniform heat flux.

The hydrodynamic boundary conditions for the current problem were as follows. The top surface was maintained at atmospheric pressure. This allowed fluid to flow into or out of the enclosure through the top surface. The left and right walls were impermeable, not allowing fluid to pass through them. The flow conditions at the bottom surface studied included both zero and nonzero normal velocity components. In this way, the effect of permeability of the bottom surface was analyzed. A more rigorous description of both thermal and hydrodynamic boundary conditions is presented in a later section.

As the porous enclosure heated up, buoyancy caused the fluid next to the heated wall to move upward. Cooler fluid then replaced the warm fluid as it moved upward after

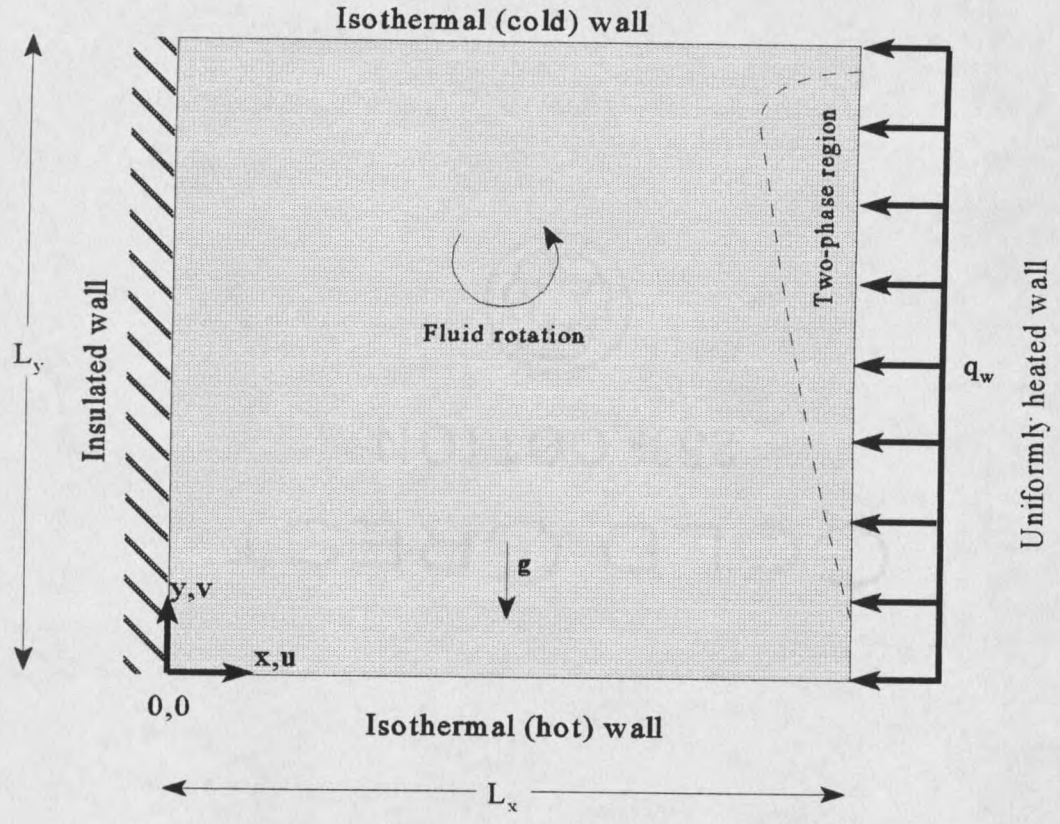

Figure 2. Geometry of Porous Enclosure Analyzed

heating and left the enclosure. Cold fluid was then drawn downward from the top permeable wall to maintain conservation of mass. Thus began a pattern of fluid motion through the enclosure. Since fluid could cross the upper permeable surface in either direction, the warm fluid adjacent to the heated wall escaped through the upper surface while cool fluid was drawn into the enclosure through the other side of the upper surface. Eventually, the fluid adjacent to the heated wall boiled and a two-phase mixture was observed.